Herpesvirus trigger accelerates neuroinflammation in a nonhuman primate model of multiple sclerosis

Emily C. Leibovitch[a], Breanna Caruso[a], Seung Kwon Ha[b], Matthew K. Schindler[b], Nathanael J. Lee[b], Nicholas J. Luciano[b], Bridgette J. Billioux[a], Joseph R. Guy[b], Cecil Yen[c], Pascal Sati[b], Afonso C. Silva[c], Daniel S. Reich[b], and Steven Jacobson[a,1]

[a]Viral Immunology Section, National Institute of Neurological Disorders and Stroke, National Institutes of Health, Bethesda, MD 20892; [b]Translational Neuroradiology Section, National Institute of Neurological Disorders and Stroke, National Institutes of Health, Bethesda, MD 20892; and [c]Cerebral Microcirculation Section, National Institute of Neurological Disorders and Stroke, National Institutes of Health, Bethesda, MD 20892

Edited by Michael B. A. Oldstone, The Scripps Research Institute, La Jolla, CA, and approved September 4, 2018 (received for review July 20, 2018)

Pathogens, particularly human herpesviruses (HHVs), are implicated as triggers of disease onset/progression in multiple sclerosis (MS) and other neuroinflammatory disorders. However, the time between viral acquisition in childhood and disease onset in adulthood complicates the study of this association. Using nonhuman primates, we demonstrate that intranasal inoculations with HHV-6A and HHV-6B accelerate an MS-like neuroinflammatory disease, experimental autoimmune encephalomyelitis (EAE). Although animals inoculated intranasally with HHV-6 (virus/EAE marmosets) were asymptomatic, they exhibited significantly accelerated clinical EAE compared with control animals. Expansion of a proinflammatory CD8 subset correlated with post-EAE survival in virus/EAE marmosets, suggesting that a peripheral (viral?) antigen-driven expansion may have occurred post-EAE induction. HHV-6 viral antigen in virus/EAE marmosets was markedly elevated and concentrated in brain lesions, similar to previously reported localizations of HHV-6 in MS brain lesions. Collectively, we demonstrate that asymptomatic intranasal viral acquisition accelerates subsequent neuroinflammation in a nonhuman primate model of MS.

marmoset | human herpesvirus 6 | EAE | multiple sclerosis | viral trigger

Multiple sclerosis (MS) is a complex autoimmune disease thought to develop in genetically susceptible individuals after exposure to specific environmental factors, including pathogens. Microbial agents have been linked to MS disease onset and exacerbations since the late 19th century (1). However, the field has largely transitioned from seeking a single causal agent toward examining ubiquitous ones that may serve as disease triggers. There has been particular focus on two human herpesviruses, Epstein-Barr virus (EBV) and human herpesvirus 6 (HHV-6) (2). Both are typically acquired during early childhood and establish latency in peripheral blood lymphocytes, lymphoid tissue, and likely the central nervous system (CNS) (3).

Several decades of research have linked HHV-6 with MS disease activity (reviewed in ref. 4). Many studies have associated the peripheral detection of HHV-6, or an immune response to HHV-6, with clinically active MS; correlations between HHV-6 antibodies and MS relapse risk or disease progression are reported across geographically varied populations. Other studies have demonstrated greater HHV-6 expression in MS brains compared with controls (5), with higher levels of viral DNA (6, 7) and mRNA (5) in demyelinated plaques. However, because MS is characterized by CNS inflammation and peripheral immune activation, it is unknown to what extent dysregulated antiviral immune responses reflect disease cause and/or effect.

HHV-6 comprises two viral species, HHV-6A and HHV-6B (8). Animal models of HHV-6 infection have been difficult to establish because rodents lack widespread expression of the main cellular receptor, CD46. Our laboratory has studied primary HHV-6 infections using the common marmoset, a small nonhuman primate (NHP), and has reported differences in antibody induction and viral detection between HHV-6A and HHV-6B, and between i.v. and intranasal routes of inoculation (9).

In humans, HHV-6 is almost ubiquitously acquired in early childhood, thereby complicating the elucidation of its role in a disease like MS, which often manifests in early adulthood. In addition to HHV-6 susceptibility, marmosets are excellent models of experimental autoimmune encephalomyelitis (EAE), an animal system used to study MS. EAE is one model of autoimmune inflammatory-mediated CNS demyelination, created by immunizing animals with CNS (usually white matter) peptides or proteins. Although EAE is typically studied in rodents, marmoset EAE presents with greater radiologic and pathologic similarities to MS, reflecting the genetic, immunological, and CNS anatomical proximity of marmosets to humans (10).

The current study, therefore, utilized marmosets to examine the effects of HHV-6 on the disease course of EAE. Consistent with evidence suggesting that viruses induce a heightened immune state (11), we observed accelerated disease in marmosets inoculated with HHV-6 compared with uninfected control animals.

Results

Characterization of HHV-6A and HHV-6B Intranasal Inoculations. In the present study, marmosets were inoculated intranasally with HHV-6A, HHV-6B, or uninfected SupT1 control material monthly for 4 mo. SupT1 is a T cell line commonly used for in vitro propagation of HHV-6. Intranasal inoculation was selected to mimic a physiologic route of infection, as humans likely acquire HHV-6, among other viruses, by this route (12). Over the 4 mo of HHV-6

Significance

Inflammatory processes drive the autoimmune disease multiple sclerosis (MS). However, what triggers this inflammation remains unknown. Several herpesviruses (HHVs), such as HHV-6 typically acquired during childhood, are associated with MS. The temporal separation between HHV-6 acquisition and MS development complicates its study as a disease trigger. Because rodents are not susceptible to HHV-6 infection, we utilized nonhuman primates to examine the impact of HHV-6 infection on an experimental MS-like disease. The viral infections were asymptomatic; however, the MS-like disease was significantly accelerated in all virally inoculated animals. Our data support the hypothesis that viruses may act as triggers to lower the threshold for autoimmunity, and warrant trials of antiviral interventions in early disease stages.

Author contributions: E.C.L. and S.J. designed research; E.C.L., B.C., S.K.H., N. J. Lee, N. J. Luciano, B.J.B., J.R.G., C.Y., and P.S. performed research; J.R.G., P.S., and A.C.S. contributed new reagents/analytic tools; E.C.L., S.K.H., M.K.S., N. J. Lee, P.S., D.S.R., and S.J. analyzed data; and E.C.L. and S.J. wrote the paper.

The authors declare no conflict of interest.

This article is a PNAS Direct Submission.

[1]To whom correspondence should be addressed. Email: jacobsons@ninds.nih.gov.

This article contains supporting information online at www.pnas.org/lookup/suppl/doi:10.1073/pnas.1811974115/-/DCSupplemental.

Published online October 15, 2018.

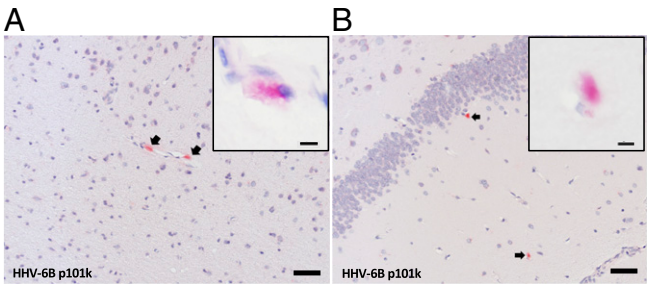

Fig. 1. HHV-6 viral antigen occasionally detected in the brain after intranasal inoculations. Two of nine examined brain regions from HHV-6B–inoculated marmoset M26 contained detectable HHV-6 late antigen p101k (red; arrows), with cytoplasmic localization. (*A*) Olfactory bulb. (*B*) Hippocampus. (Scale bar: 50 μm; *Inset* scale bar: 5 μm.)

intranasal inoculations, marmosets were weighed twice weekly and monitored for clinical symptoms by in-cage observation and out-of-cage examinations. Throughout the period of intranasal inoculations with either virus, no clinical symptoms were observed. This is consistent with our prior study, in which no symptoms were observed in marmosets intranasally inoculated with HHV-6A (9).

To determine whether marmosets mounted HHV-6 antibody responses to the intranasal inoculations, plasma was evaluated for HHV-6–specific IgG. HHV-6 antibody responses were observed in three of four HHV-6B–inoculated marmosets, one of four HHV-6A–inoculated marmosets, and none of the controls. Saliva and peripheral blood mononuclear cells (PBMCs) were collected every 2 wk and evaluated for viral DNA by HHV-6 species-specific droplet digital PCR (13). Viral DNA was detected in the saliva of all four HHV-6B–inoculated marmosets at multiple time points. By contrast, viral DNA was never detected in the saliva of HHV-6A inoculated marmosets, supporting the idea of distinct cellular tropisms for HHV-6A and HHV-6B (8). Viral DNA was not detected in PBMCs from either group (*SI Appendix*, Fig. S1).

The HHV-6B–inoculated marmoset M26 was euthanized shortly after the intranasal inoculations due to a wasting disease not uncommon in captive marmoset colonies. This afforded us the opportunity to determine whether HHV-6B intranasal inoculation resulted in detectable virus in the brain. The entire brain was sectioned and surveyed by immunohistochemistry using three HHV-6 antibodies validated for this study (only staining with HHV-6B–specific p101k is shown). Low levels of HHV-6 reactivity were detected in a few regions (two of nine slabs), including the frontal cortex/olfactory bulb and hippocampus (Fig. 1). When present, viral antigen was detectable in multiple adjacent sections. B cells were undetected, while T cell infiltrates were observed in some vessels.

Virus-Inoculated Marmosets Exhibit Accelerated Clinical EAE. To assess the effects of a preexisting viral infection in the context of neuroinflammation, all marmosets were induced with EAE 2 mo after the last HHV-6 intranasal inoculation ($n = 11$). We hypothesized that the HHV-6–inoculated marmosets (virus/EAE) would develop more severe disease compared with the SupT1 control–inoculated marmosets (control/EAE).

Marmosets were monitored clinically and radiologically until predetermined clinical end points. A significantly shorter time to EAE symptom onset was observed in the virus/EAE groups compared with the controls (Fig. 2*A*; $P = 0.04$). Common early symptoms included apathy, dyscoordination, visual disturbances, and/or greater than 10% weight loss. Notably, in addition to a shorter time to symptom onset, virus/EAE marmosets survived for a significantly shorter period following EAE induction ($P = 0.03$) (Fig. 2*B*), with no differences between the HHV-6A and HHV-6B groups. One control marmoset developed only mild symptoms, and never met clinical end points for euthanasia (M33, see *SI Appendix*, Table S1).

More Severe Radiologic Disease in Virus/EAE Marmosets. Due to its sensitivity and noninvasiveness, MRI is central to the monitoring of MS lesions. In marmoset EAE, MRI-visible lesions develop throughout the CNS and can be followed over time. Like MS brain lesions, marmoset EAE brain lesions are venocentric (14) and exhibit similar compositions of inflammatory infiltrates (15), suggesting shared pathophysiologic mechanisms. After EAE induction, marmosets underwent in vivo brain MRI every 2 wk. There was a nonsignificant trend for earlier lesion onset in virus/EAE compared with control/EAE marmosets (41 ± 14 d versus 63 ± 45 d, respectively). In all marmosets, lesions were visible predominantly in the white matter tracts; there were no apparent differences in lesion location between the groups. There were no differences in cumulative lesion number or lesion volume between the virus/EAE and control/EAE groups.

Multiple types of scans were run during each imaging session to assess EAE lesion dynamics and evolution. White matter lesions appear hyperintense on proton density (PD)-weighted scans (Fig. 3*A*) and hypointense on T1-weighted scans (Fig. 3*B*). Final cumulative PD and T1 brain lesion volumes are shown for each marmoset in Fig. 3*C*. All brain lesions were detectable by PD-weighted scans, while only a subset was detectable by T1-weighted scans. The mean survival time for the virus/EAE marmosets was 18 d after PD lesion onset (Fig. 3*D*) and 9 d after T1 lesion onset (Fig. 3*E*), both significantly shorter than the control group. When the T1 lesion burden as a proportion of total lesion volume was compared across groups, the HHV-6B animals showed a significantly greater mean fraction compared with the HHV-6A or control animals (one-way ANOVA, $P = 0.05$).

HHV-6 Viral Antigen Is Up-Regulated in Inflammatory EAE Brain Lesions. To determine whether viral antigen could be detected in brain tissue, HHV-6 immunohistochemistry was performed on

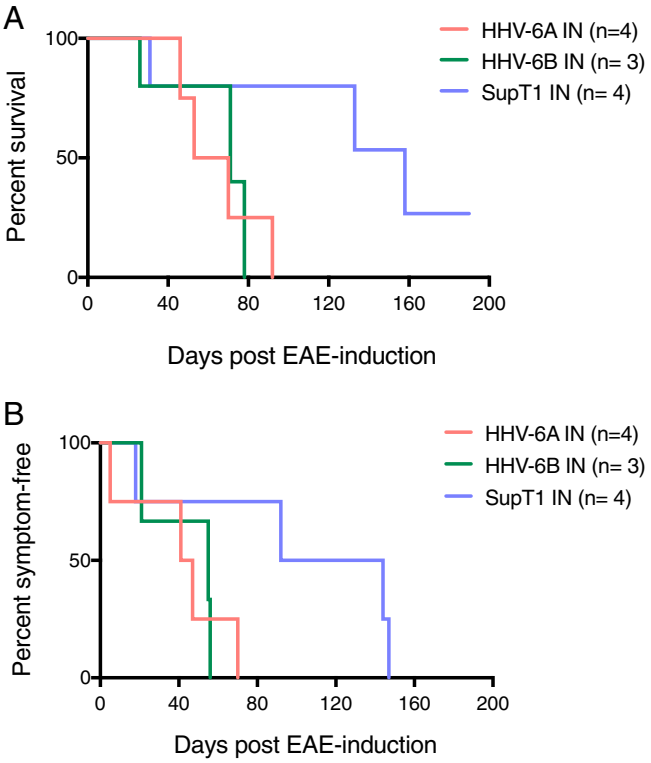

Fig. 2. Significantly accelerated clinical EAE in HHV-6 intranasally inoculated marmosets. (*A*) Reduced time to symptom onset in virus/EAE marmosets compared with SupT1 control/EAE marmosets (unpaired *t* test, $P = 0.04$). (*B*) Shortened survival post-EAE induction in virus/EAE marmosets compared with SupT1 control/EAE marmosets (unpaired *t* test, $P = 0.03$).

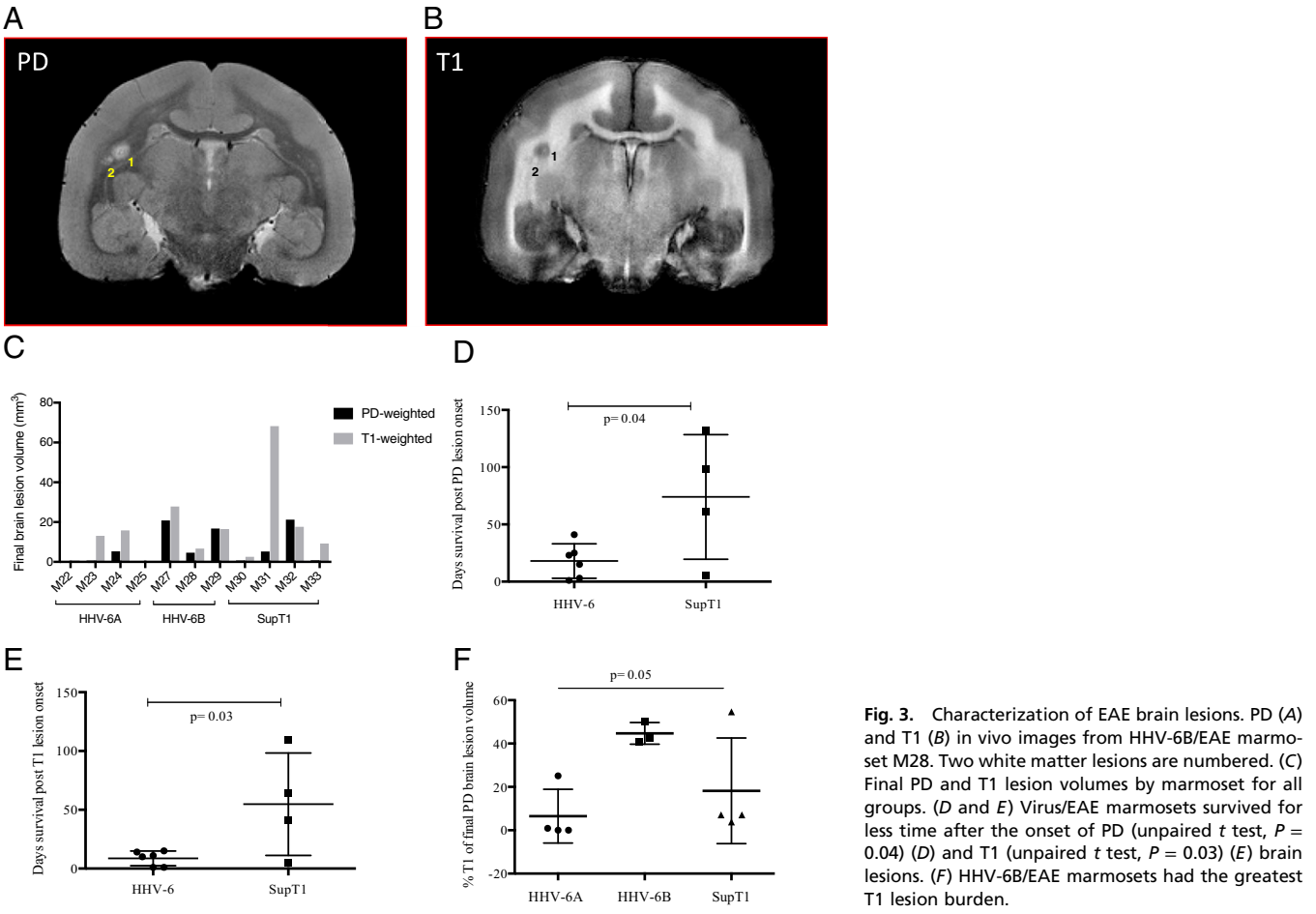

Fig. 3. Characterization of EAE brain lesions. PD (*A*) and T1 (*B*) in vivo images from HHV-6B/EAE marmoset M28. Two white matter lesions are numbered. (*C*) Final PD and T1 lesion volumes by marmoset for all groups. (*D* and *E*) Virus/EAE marmosets survived for less time after the onset of PD (unpaired *t* test, $P = 0.04$) (*D*) and T1 (unpaired *t* test, $P = 0.03$) (*E*) brain lesions. (*F*) HHV-6B/EAE marmosets had the greatest T1 lesion burden.

CNS tissues from all HHV-6B virus/EAE marmosets when clinical end points were reached. Viral antigen was up-regulated in inflammatory, subcortical white matter lesions from a representative virus/EAE marmoset (Fig. 4 *A* and *B*). These lesions are 2 to 4 wk old, estimated by time of appearance on in vivo MRI. Viral antigen was also detected in the leptomeninges around the hippocampal fissure (Fig. 4*C*). HHV-6 antigen was additionally localized to the choroid plexus, which has been described as a cerebrospinal fluid gateway for immune cells trafficking into the CNS (16). This is in contrast to the animal infected with HHV-6 but not induced with EAE, in which viral antigen was sparsely detected in the brain (Fig. 1). Control/EAE brain sections did not stain for HHV-6.

Additional immunohistochemistry was performed to characterize the cellular composition of HHV-6–positive lesions (Fig. 5), which tended to be intensely inflamed. Serial sections from a representative 2- to 4-wk-old HHV-6–positive lesion are shown in Fig. 5*A*. This lesion shows a high degree of lymphocyte infiltration, with dispersion into the parenchyma. There is moderate staining for myeloid-related protein 14 (MRP14), expressed on recently infiltrating monocytes and macrophages during early acute inflammation. MRP14 is less tightly perivascular than the lymphocyte markers or Iba-1. Iba-1 is expressed on both microglia and macrophages and shows dense staining in both the perivascular cuff and surrounding parenchyma. This lesion also stains for fibrinogen, a marker of blood-brain barrier leakiness (17). The absence of myelin proteolipid protein (PLP) indicates early-stage demyelination.

Colocalization studies were performed to determine which cells within the inflammatory HHV-6B/EAE lesion expressed HHV-6. As shown in Fig. 5*B* by double-staining immunohistochemistry, there was a marked colocalization of HHV-6–positive (brown) and CD3-positive (blue) cells. Immunofluorescence studies confirmed these findings (Fig. 5 *C*–*E*). These findings are consistent with the known T cell tropism of HHV-6B (18) and suggest that the up-regulation of HHV-6 in EAE lesions resulted from increased immune cell trafficking known to occur in the early stages of lesion formation. Increased HHV-6 expression in inflammatory lesions of virus-infected/EAE animals relative to the surrounding parenchyma mirrors the observations of HHV-6 in MS lesions (19–21).

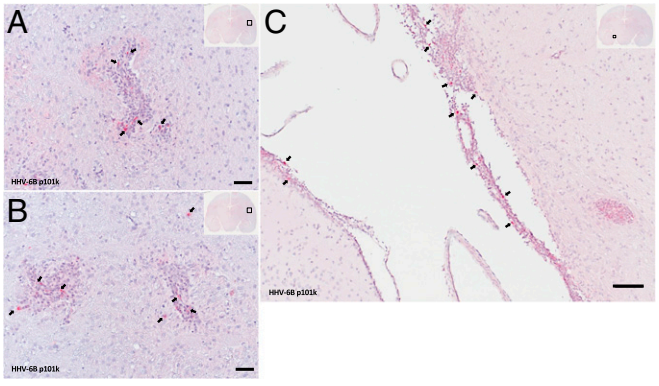

Fig. 4. HHV-6 viral antigen is up-regulated in virus/EAE marmoset brains. Arrows indicate positivity for HHV-6 late antigen p101k (red) in inflamed brain regions from representative virus/EAE marmoset M28. (*A* and *B*) Temporal white matter around putamen. (*C*) Leptomeninges around hippocampal fissure. (Scale bar: 50 μm.)

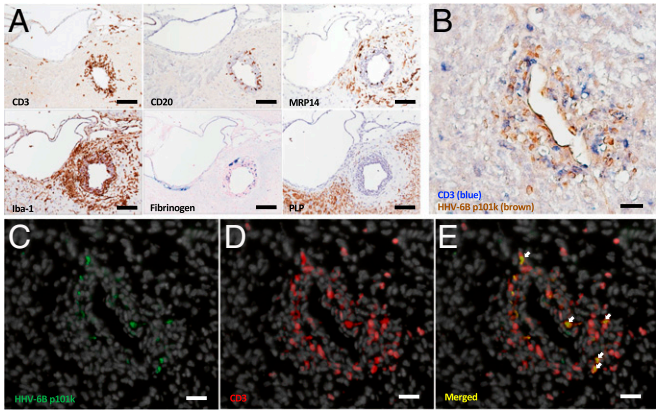

Fig. 5. Characterization of HHV-6–positive brain lesions from a virus/EAE marmoset. (*A*) Serial sections of an HHV-6–positive perivascular EAE lesion demonstrate CD3 T and CD20 B cell infiltrates, MRP14$^+$ macrophages/monocytes, Iba-1$^+$ microglia, blood-brain barrier leakiness evidenced by fibrinogen deposition, and demyelination evidenced by the absence of myelin PLP. (Scale bar: 100 μm.) (*B*) HHV-6 antigen (brown) colocalizes with CD3 T cells (blue). (*C*) HHV-6–infected cells in green (Alexa 488). (*D*) CD3 T cells in red (Alexa 594), with DAPI counterstain (gray). (*E*) Merged image with arrows showing colocalization of HHV-6 viral antigen with CD3 T cells. (Scale bar: *B*–*E*, 50 μm.) The lesion pictured in *A* is located in the gray matter (lateral dorsal thalamic nucleus), whereas the lesion pictured in *B*–*E* is located in the temporal white matter. Lesions are from HHV-6B/EAE marmoset M28.

CD8 E/M Expansion in Virus/EAE Marmosets Correlates with Disease Duration. To characterize the mechanism of accelerated disease in the virus/EAE marmosets, PBMCs were immunophenotyped by flow cytometry pre- and post-EAE induction. T cell subpopulation definitions were based on a prior NHP study (22): naïve ($CD3^+CD27^+CD45RA^+$), effector ($CD3^+CD27^-CD45RA^+$), effector/memory ($CD3^+CD27^-CD45RA^-$), and memory ($CD3^+CD27^+CD45RA^-$) (Fig. 6*A*). As shown in the histogram of Fig. 6*A*, the effector/memory subpopulation (blue peak) produced the greatest amount of IFN-γ, supporting this immunophenotyping scheme.

In the virus/EAE marmosets, a decrease in naïve CD8 cells and an increase in effector/memory CD8 cells were observed at the terminal EAE time point, which varied between animals. No such trends were observed in the control/EAE marmosets (representative plots shown in Fig. 6*B*). Further, we observed that the reduction in naïve CD8 cells and the increase in effector/memory CD8 cells significantly correlated with EAE duration in the virus/EAE marmosets (Fig. 6 *C* and *D*), but not the control/EAE marmosets (Fig. 6 *E* and *F*). These data suggest that the accelerated disease observed in the virus/EAE groups may have been related to an expansion of proinflammatory, IFN-γ–producing CD8 T cells.

Discussion

While no particular infectious agent has been demonstrated to trigger MS onset, many have been suspected (23). The focus in recent decades has shifted to several ubiquitous herpesviruses, particularly EBV and HHV-6. To model an MS-like disease in the context of a viral infection, we utilized small NHPs, which are both susceptible to HHV-6 (9) and well-characterized models of EAE (24). In the present study, HHV-6 was administered intranasally to mimic a physiologic route of infection. HHV-6, along with other neurotropic viruses, is thought to access the CNS via the olfactory pathway, as the olfactory neuroepithelium provides a direct route from the periphery to the brain. Interestingly, an early clinical manifestation of MS is olfactory dysfunction (25).

Several observations of HHV-6–infected marmosets are comparable to what has been reported in humans. Similar to the majority of HHV-6 infections that occur in early childhood, marmosets inoculated intranasally with HHV-6A or HHV-6B were asymptomatic. In humans, HHV-6B is detected far more frequently in saliva than HHV-6A (13, 26). Likewise, in this study, viral DNA was detected in the saliva of all HHV-6B–inoculated marmosets and none of the HHV-6A inoculated marmosets. Lastly, following the intranasal inoculations, low levels of viral antigen were detectable in the olfactory bulb and hippocampus of an HHV-6B–infected marmoset. In humans, low levels of HHV-6 are observed in normal CNS tissues (27), suggestive of a viral reservoir. Moreover, HHV-6 is reportedly tropic for limbic structures of the human CNS, reflected by its association with encephalitis (28) and epilepsy (29).

A major finding in this study is that marmosets inoculated with HHV-6, although asymptomatic, exhibited significantly accelerated clinical EAE compared with nonvirally inoculated controls. This was supported by clinical, radiological, and histopathological outcomes. Clinically, virus/EAE marmosets had significantly earlier symptom onset, more progressive disease, and significantly shortened survival compared with control/EAE animals.

Inflammatory lesions that develop in the marmoset EAE model are distributed throughout the CNS and can be followed by MRI due to the size and structure of the marmoset brain (30). Virus/EAE marmosets trended toward earlier development of lesions and an increased lesion load compared with controls. Despite the small numbers of animals per group, the HHV-6B–inoculated marmosets exhibited an increased proportion of T1 lesions compared with the HHV-6A group. Given the acute lesions in the virus/EAE marmosets, we hypothesize that this T1 hypointensity represents a combination of inflammation (edema) and tissue destruction of varying degrees (15, 17). In humans, HHV-6B, relative to HHV-6A, tends to be associated with acute inflammatory events such as seizures and encephalitis (29). By histopathology, virus/EAE marmosets had a greater number of acute inflammatory lesions compared with control/EAE animals.

Early studies reporting the localization of HHV-6 to MS brain lesions provided strong rationale for further studies of HHV-6 in MS pathogenesis (31). In the brains of virus/EAE marmosets, viral antigen was far more frequently detected, relative to the virus-inoculated marmoset not induced with EAE. Specifically, viral antigen was localized to sites of inflammatory lesion formation and colocalized with CD3 T cells, consistent with the known T cell lymphotropism of HHV-6 (32). In studies of normal human brains, HHV-6 is detected at low levels (3, 27), whereas in MS brains, higher levels of virus can be demonstrated in lesions (6, 7). Similarly, HHV-6–infected marmosets had little detectable viral antigen in the CNS, which dramatically increased after EAE induction. In this study, HHV-6 staining was performed using an antibody specific to a structural protein of the viral tegument, therefore suggesting an active (versus latent) infection.

In MS and marmoset EAE, brain lesions are perivascular and tissue damage results from the dispersion of inflammatory infiltrates from a central vessel into the neighboring parenchyma. Blood-brain barrier permeability is a key step in lesion formation (15) and has been shown to be promoted by peripheral immune activation. We therefore hypothesized that the accelerated disease in the virus/EAE marmosets reflected peripheral immune activation resulting from the intranasal viral inoculations. Peripheral T cell subpopulation analysis revealed a significant correlation between effector/memory CD8 T cells and time post-EAE induction in the virus/EAE marmosets, but not in the control/EAE marmosets. We hypothesize that the intranasal viral inoculations primed these (virus-specific?) cells, which then expanded after EAE induction and contributed to the accelerated disease observed in the virus/EAE groups.

Various mechanisms have been proposed to explain how strong immune responses elicited by microorganisms might contribute to immune-mediated disease, particularly autoimmunity. An example of a direct mechanism is molecular mimicry, which occurs when structural similarities between viral and self-antigens result in cross-reactive immune responses. An example of an indirect mechanism is bystander activation, which occurs when microorganisms nonspecifically activate (autoreactive?) cells in the microenvironment (11). These mechanisms are not mutually exclusive. The fertile field hypothesis addresses how these mechanisms, among others, may

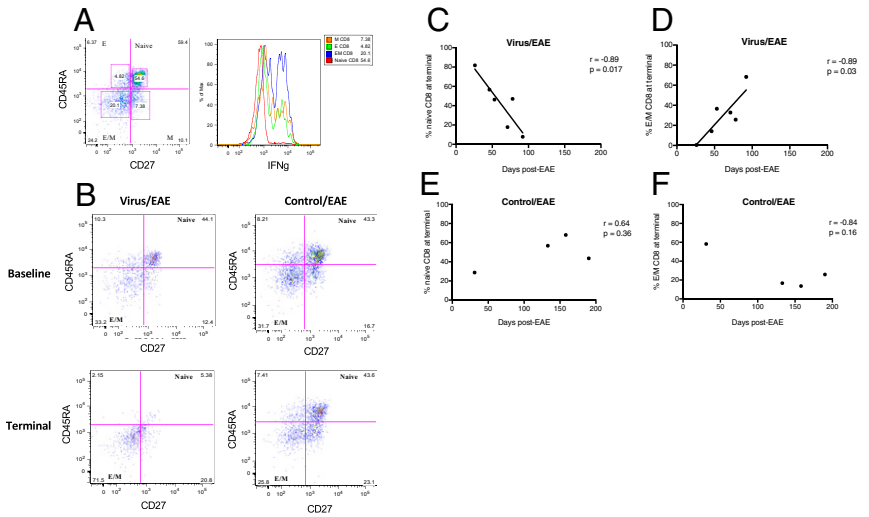

Fig. 6. Increase in IFN-γ–producing effector/memory (E/M) CD8 T cells significantly correlates with disease duration in virus-inoculated marmosets. (*A*) Representative flow cytometry plot of $CD8^+$ CD45RA/CD27 T cell subsets, with histogram showing highest IFN-γ production by E/M subset. E, effector; M, memory. (*B*) Representative flow cytometry plots showing a decrease in naïve $CD8^+$ T cells at terminal EAE time points in virus/EAE, but not control/EAE, marmosets. (*C* and *D*) Contraction of naïve CD8 (*C*) and expansion of E/M CD8 (*D*) T cells correlate with EAE disease duration in virus-inoculated marmosets. (*E* and *F*) In the control/EAE marmosets, no such correlation was observed for either the naïve CD8 (*E*) or the E/M CD8 (*F*) subset.

synergize to culminate in autoimmunity. According to this hypothesis, a fertile field conceptualizes a heightened immune state induced by infections, which is regulated by a balance between the infection quality (magnitude, timing, and context) and the host immune response to infection. In the presence of viral, self-, or other antigens, such a heightened immune state sets the stage for the expansion of autoreactive cells, thus resulting in a lowered threshold for autoreactivity (11).

Several groups have previously shown that viral prime/challenge models in rodents result in accelerated rodent EAE (33–35). Moreover, others have demonstrated that viral infection of the CNS can either prime disease development in challenge models in which the challenge alone rarely induces disease (36) or increase EAE susceptibility in animals that are normally somewhat resistant (37). Observations from our study using an NHP model provide empirical evidence that a viral infection of the periphery or CNS can result in an enhanced response to a subsequent autoimmune challenge, thus supporting the long-standing idea that virus(es) may act as triggers in MS or other inflammatory-mediated neurologic conditions.

Materials and Methods

Experimental Design. Ten unrelated adult marmosets and one twin pair were used in this study ($n = 12$). Animals were randomly assigned to the HHV-6A, HHV-6B, and uninfected SupT1 control groups. Each group was age matched (38 ± 11 mo) with three females and one male, to reflect the sex ratio of MS prevalence, estimated from 2.3:1 to 3.5:1 (38). Marmosets were intranasally inoculated with 10^8 viral copies of HHV-6A, HHV-6B, or equivalent volumes of uninfected SupT1 monthly for 4 mo. Two months later, 11 of 12 marmosets were induced with EAE. After EAE induction, in vivo brain MRI was performed every 2 wk until predefined clinical end points.

Animal Ethics and Housing. Experiments adhered to active protocols (1308-12 and 1308-15) approved by the National Institute of Neurological Disorders and Stroke Institutional Animal Care and Use Committee. All marmosets were pair-housed when possible, at NIH facilities (PHS Assurance #A4149-01) in accordance with the standards of the American Association for Accreditation of Laboratory Animal Care.

HHV-6 Propagation and Marmoset Inoculations. HHV-6B Z29 was propagated in SupT1 cells, and HHV-6A GS was propagated in HSB-2 cells. Infections were monitored for cytopathic effects, and viral loads were monitored by PCR. Supernatants were frozen at −80 °C and thawed immediately before the inoculations. Supernatants (<200-μL volumes) were administered dropwise into alternating nostrils of sedated marmosets via a 1-mL syringe fitted with a 27-gauge needle covered with a small piece of polyethylene (PE20) tubing.

EAE Induction. Each marmoset was injected intradermally with 200 mg of human white matter homogenate, emulsified with 250 μL of incomplete Freund adjuvant (Difco Laboratories) containing 1.8 mg of desiccated heat-killed *Mycobacterium tuberculosis* as previously described (24).

Marmoset Clinical Monitoring. Clinical assessments were scored using a modified version of a semiquantitative scale used for marmoset EAE (39): 0, no clinical signs; 0.5, apathy or altered walking pattern without ataxia; 1, lethargy or weight loss exceeding 10%; 1.5, tremor or loss of tail tone; 2, ataxia, sensory loss, or optic disease; 2.25, monoparesis; 2.5, paraparesis or sensory loss; and 3, paraplegia or hemiplegia. Marmosets were weighed twice weekly and killed when a clinical score of 3 was sustained for 24 h.

Blood and Saliva Collection. Blood and saliva were collected every 2 wk for the duration of the study. Approximately 1 mL of venous blood was fractioned into PBMCs and plasma, and stored until use. Saliva was collected by swabbing the oral mucosa of anesthetized marmosets. Saliva-saturated gauze was spun for 5 min at 9,600 × *g* and stored at −20 °C until use.

DNA Extraction and PCR. DNA was extracted from saliva, PBMCs, or tissue using a DNeasy blood and tissue DNA extraction kit (Qiagen) according to the manufacturer's specifications. Droplet digital PCR was used to amplify HHV-6A and HHV-6B *u57* and the marmoset housekeeping gene *beta actin*. PCR was performed as previously described (13). The HHV-6 primers and probes have been previously reported (13). The marmoset *beta actin* sequences are as follows: forward AGGCGCACAGTAGGTCTGAA, reverse GCGTACAAGGAAAGCACAGC, VIC-MGBNFQ probe CCCCATCCCAAGACCCCA.

Antibody Assays. Marmoset plasma antibodies against HHV-6 were measured using electrochemiluminescence technology (Meso Scale Diagnostics). Antigens were spotted onto high bind plates as previously described (40). Plasma was added in duplicate at a final dilution of 1:10. SULFO-TAG–labeled anti-human/NHP IgG was used as a secondary antibody. HHV-6 reactivity is corrected for SupT1 lysate reactivity.

Marmoset ex Vivo PBMC Stimulations. Marmoset PBMCs were plated at a concentration of 3×10^6 to 5×10^6 cells per 100 μL in a 96-well round-bottom plate, with the addition of anti-human CD28 (1 μg/mL) and anti-human CD49d (1 μg/mL). Cells were incubated overnight with phorbol 12-myristate 13-acetate (5 ng/mL) and ionomycin (500 ng/mL). Golgi Plug (0.2 ng) and Golgi Stop (0.1 ng) were added for 5 h in a 37 °C 5% CO_2 incubator.

Extracellular antibodies included CD3 APC-Cy7 (clone SP34-2), CD4 BV510 (clone L200), CD8 APC (clone LT8), CD56 PE-Cy7 (clone NCAM16.2), CD45RA V450 (clone 5H9), and CD27 PerCP-Cy5.5 (clone M-T271). Cells were fixed, permeabilized, and stained with IFN-γ FITC (clone MD-1; U-CyTech Biosciences). Samples were run in 96-well plates using a BD LSR II High Throughput Sampler. Data analysis was performed using FlowJo version 8.8.6.

In Vivo Brain MRI. In vivo imaging was performed in a 7T/30 cm Bruker scanner using a custom-made eight-channel surface coil as previously described (15, 41). All marmosets were scanned before the first viral inoculation, before EAE induction, and every 2 wk after EAE induction until clinical end points were met. All scans were acquired with whole brain coverage over 66 slices. In vivo MRI parameters are given in *SI Appendix*, Table S2.

Euthanasia. Transcardial perfusion with cold 4% paraformaldehyde (PFA) was performed as previously described (9, 15), and CNS tissues were collected. The brain was fixed in 10% neutral buffered formalin and the spinal cord was fixed in 4% PFA for up to 2 wk before transfer to an MRI-invisible fluid (Fomblin; Solvay S.A.). Samples of non-CNS tissues were snap frozen and assessed for HHV-6 viral DNA.

Histopathology. Postmortem images of each marmoset brain were used to create individualized 3D-printed brain models as previously described (42), to enable precise correspondence between MRI and histopathology. Lesions of interest were identified on the postmortem MRI, the brain was sliced into 8 to 10 sections, and each slice was paraffin-embedded (Histoserv). Slices were sectioned at 4 μm and stained with hematoxylin and eosin. Immunoperoxidase staining was used for Iba1, MRP14, CD3, CD20, and PLP, while alkaline phosphatase staining was used for HHV-6 and fibrinogen. Histopathological methods have been previously described (17).

Three HHV-6 antibodies were validated for use in this study: DR6/7 (clone 33B12; NIH AIDS Reagent program), p41 (clone 3E3; Applied Biological Materials, Inc.), and 101 kDa (clone C3108-103; Millipore). DR6/7 is the direct repeat 6 (DR6) gene, previously called DR7; p41 encodes a viral DNA processivity factor; and 101 kDa is a major structural antigen/tegument protein that is reportedly specific for HHV-6B and likely exhibits nuclear localization early in infection and cytoplasmic localization later in infection (43). Only staining with 101 kDa is shown. Images were taken using a Zeiss Observer 1 microscope (Zeiss) and ZEN blue software (Zeiss). All sections were analyzed by a veterinary pathologist.

Statistical Analyses. All data were analyzed using Prism 6 (GraphPad Software, Inc.). Values are written as mean ± SD, unless otherwise noted. One-way ANOVA was used for multiple group comparisons, and linear regression analyses were used to evaluate flow cytometry data. Statistical significance was reached with a P value less than 0.05.

ACKNOWLEDGMENTS. We thank Sam Antonio, Oscar Chevez-Quintanilla, and Dr. James O'Malley (National Institute of Neurological Disorders and Stroke animal health care section) for outstanding marmoset caretaking; Lisa Zhang and Xiaozhen Li for assistance with marmoset in vivo MRI; and Dr. David Hudnall (Yale University) for HHV-6 immunohistochemistry expertise.

1. Compston A, Lassman H, McDonald I (2006) The story of multiple sclerosis. *McAlpine's Multiple Sclerosis*, (Churchill Livingstone/Elsevier, London), 4th Ed.
2. Virtanen JO, Jacobson S (2012) Viruses and multiple sclerosis. *CNS Neurol Disord Drug Targets* 11:528–544.
3. Merelli E, et al. (1997) Human herpes virus 6 and human herpes virus 8 DNA sequences in brains of multiple sclerosis patients, normal adults and children. *J Neurol* 244: 450–454.
4. Leibovitch EC, Jacobson S (2014) Evidence linking HHV-6 with multiple sclerosis: An update. *Curr Opin Virol* 9:127–133.
5. Opsahl ML, Kennedy PG (2005) Early and late HHV-6 gene transcripts in multiple sclerosis lesions and normal appearing white matter. *Brain* 128:516–527.
6. Cermelli C, et al. (2003) High frequency of human herpesvirus 6 DNA in multiple sclerosis plaques isolated by laser microdissection. *J Infect Dis* 187:1377–1387.
7. Sanders VJ, Felisan S, Waddell A, Tourtellotte WW (1996) Detection of herpesviridae in postmortem multiple sclerosis brain tissue and controls by polymerase chain reaction. *J Neurovirol* 2:249–258.
8. Ablashi D, et al. (2014) Classification of HHV-6A and HHV-6B as distinct viruses. *Arch Virol* 159:863–870.
9. Leibovitch E, et al. (2013) Novel marmoset (Callithrix jacchus) model of human herpesvirus 6A and 6B infections: Immunologic, virologic and radiologic characterization. *PLoS Pathog* 9:e1003138.
10. 't Hart BA, et al. (2000) A new primate model for multiple sclerosis in the common marmoset. *Immunol Today* 21:290–297.
11. von Herrath MG, Fujinami RS, Whitton JL (2003) Microorganisms and autoimmunity: Making the barren field fertile? *Nat Rev Microbiol* 1:151–157.
12. Harberts E, et al. (2011) Human herpesvirus-6 entry into the central nervous system through the olfactory pathway. *Proc Natl Acad Sci USA* 108:13734–13739.
13. Leibovitch EC, et al. (2014) Coinfection of human herpesviruses 6A (HHV-6A) and HHV-6B as demonstrated by novel digital droplet PCR assay. *PLoS One* 9:e92328.
14. Gaitán MI, et al. (2013) Perivenular brain lesions in a primate multiple sclerosis model at 7-tesla magnetic resonance imaging. *Mult Scler* 20:64–71.
15. Maggi P, et al. (2014) The formation of inflammatory demyelinated lesions in cerebral white matter. *Ann Neurol* 76:594–608.
16. Wilson EH, Weninger W, Hunter CA (2010) Trafficking of immune cells in the central nervous system. *J Clin Invest* 120:1368–1379.
17. Lee NJ, et al. (2018) Spatiotemporal distribution of fibrinogen in marmoset and human inflammatory demyelination. *Brain* 141:1637–1649.
18. De Bolle L, Van Loon J, De Clercq E, Naesens L (2005) Quantitative analysis of human herpesvirus 6 cell tropism. *J Med Virol* 75:76–85.
19. Challoner PB, et al. (1995) Plaque-associated expression of human herpesvirus 6 in multiple sclerosis. *Proc Natl Acad Sci USA* 92:7440–7444.
20. Goodman AD, Mock DJ, Powers JM, Baker JV, Blumberg BM (2003) Human herpesvirus 6 genome and antigen in acute multiple sclerosis lesions. *J Infect Dis* 187: 1365–1376.
21. Knox KK, Harrington DP, Carrigan DR (1995) Fulminant human herpesvirus six encephalitis in a human immunodeficiency virus-infected infant. *J Med Virol* 45: 288–292.
22. Sicard H, et al. (2005) In vivo immunomanipulation of V gamma 9V delta 2 T cells with a synthetic phosphoantigen in a preclinical nonhuman primate model. *J Immunol* 175:5471–5480.
23. Venkatesan A, Johnson RT (2014) Infections and multiple sclerosis. *Handbook of Clinical Neurology*, ed Goodin DS (Elsevier, Amsterdam), Vol 122.
24. Massacesi L, et al. (1995) Active and passively induced experimental autoimmune encephalomyelitis in common marmosets: A new model for multiple sclerosis. *Ann Neurol* 37:519–530.
25. Lucassen EB, Turel A, Knehans A, Huang X, Eslinger P (2016) Olfactory dysfunction in multiple sclerosis: A scoping review of the literature. *Mult Scler Relat Disord* 6:1–9.
26. Akhyani N, et al. (2000) Tissue distribution and variant characterization of human herpesvirus (HHV)-6: Increased prevalence of HHV-6A in patients with multiple sclerosis. *J Infect Dis* 182:1321–1325.
27. Lin CT, Leibovitch EC, Almira-Suarez MI, Jacobson S (2016) Human herpesvirus multiplex ddPCR detection in brain tissue from low- and high-grade astrocytoma cases and controls. *Infect Agent Cancer* 11:32.
28. Hill JA, et al. (2012) Cord-blood hematopoietic stem cell transplant confers an increased risk for human herpesvirus-6-associated acute limbic encephalitis: A cohort analysis. *Biol Blood Marrow Transplant* 18:1638–1648.
29. Theodore WH, et al. (2008) Human herpes virus 6B: A possible role in epilepsy? *Epilepsia* 49:1828–1837.
30. Sati P, et al. (2012) In vivo quantification of T_2 anisotropy in white matter fibers in marmoset monkeys. *Neuroimage* 59:979–985.
31. Knox KK, Brewer JH, Henry JM, Harrington DJ, Carrigan DR (2000) Human herpesvirus 6 and multiple sclerosis: Systemic active infections in patients with early disease. *Clin Infect Dis* 31:894–903.
32. Lusso P, et al. (1988) In vitro cellular tropism of human B-lymphotropic virus (human herpesvirus-6). *J Exp Med* 167:1659–1670.
33. Casiraghi C, Márquez AC, Shanina I, Horwitz MS (2015) Latent virus infection upregulates CD40 expression facilitating enhanced autoimmunity in a model of multiple sclerosis. *Sci Rep* 5:13995.
34. Casiraghi C, et al. (2012) Gammaherpesvirus latency accentuates EAE pathogenesis: Relevance to Epstein-Barr virus and multiple sclerosis. *PLoS Pathog* 8:e1002715.
35. Peacock JW, Elsawa SF, Petty CC, Hickey WF, Bost KL (2003) Exacerbation of experimental autoimmune encephalomyelitis in rodents infected with murine gammaherpesvirus-68. *Eur J Immunol* 33:1849–1858.
36. Libbey JE, Fujinami RS (2010) Potential triggers of MS. *Results Probl Cell Differ* 51: 21–42.
37. Massanari RM, Paterson PY, Lipton HL (1979) Potentiation of experimental allergic encephalomyelitis in hamsters with persistent encephalitis due to measles virus. *J Infect Dis* 139:297–303.
38. Harbo HF, Gold R, Tintoré M (2013) Sex and gender issues in multiple sclerosis. *Ther Adv Neurol Disorder* 6:237–248.
39. Jagessar SA, et al. (2012) Unravelling the T-cell-mediated autoimmune attack on CNS myelin in a new primate EAE model induced with MOG34-56 peptide in incomplete adjuvant. *Eur J Immunol* 42:217–227.
40. Yao K, et al. (2009) Detection of human herpesvirus-6 in cerebrospinal fluid of patients with encephalitis. *Ann Neurol* 65:257–267.
41. Papoti D, et al. (2017) Design and implementation of embedded 8-channel receive-only arrays for whole-brain MRI and fMRI of conscious awake marmosets. *Magn Reson Med* 78:387–398.
42. Luciano NJ, et al. (2016) Utilizing 3D printing technology to merge MRI with histology: A protocol for brain sectioning. *J Vis Exp*, 10.3791/54780.
43. Takemoto M, et al. (2005) Human herpesvirus 6 open reading frame U14 protein and cellular p53 interact with each other and are contained in the virion. *J Virol* 79: 13037–13046.